J. Appl. Comput. Mech., 8(3) (2022) 1065-1075
DOI: 10.22055/jacm.2022.38834.3292

ISSN: 2383-4536
jacm.scu.ac.ir

Shahid Chamran University of Ahvaz

Journal of Applied and Computational Mechanics

Research Paper

Two-dimensional Stress and strain Analysis for Graphene-polymer Nanocomposite under Axial Load

Tatyana Petrova[1], Elisaveta Kirilova[1], Wilfried Becker[2], Jordanka Ivanova[3]

[1] Institute of Chemical Engineering, Bulgarian Academy of Sciences, Acad. G. Bonchev str., Bl.103, Sofia 1113, Bulgaria, Email: t.petrova@iche.bas.bg

[2] Institute of Structural Mechanics, TU Darmstadt, Franziska-Braun-Str. 7, L5|01 347a, 64287 Darmstadt, Germany, Email: becker@fsm.tu-darmstadt.de

[3] European Polytechnic University, Sv. Sv. Kiril i Metodiy Str. 23, Pernik 2300, Bulgaria, Email: ivanovajordanka@yahoo.com

Received October 12 2021; Revised January 11 2022; Accepted for publication February 26 2022.
Corresponding author: T. Petrova (tancho66@yahoo.com; t.petrova@iche.bas.bg)

Abstract. A two-dimensional stress-function method describing the stress transfer in a three-layered adhesive bonded graphene and poly(methyl methacrylate) nanocomposite structure, subjected to axial load is developed and applied. The governing ordinary differential equation of fourth order with constant coefficients for the axial stress in the first layer is obtained minimizing the strain energy in the whole structure and solved analytically. The two-dimensional stresses and strains (axial, shear and peel) in the structure's layers are expressed and calculated as functions of this axial one and its derivatives and illustrated with graphics. The model graphene strain is compared with experimental data for strain in graphene and shear-lag model results from literature and shows good agreement at 0.4% external strains.

Keywords: Graphene-SU8-polymethyl methacrylate (PMMA), axial tension, two-dimensional stress-function method, analytical solution.

1. Introduction

In recent years, potential graphene applications include various medical, chemical and industrial processes enhanced or enabled by the use of new graphene materials. Graphene chemical durability, thermal stability, and high mechanical strength make it suitable for harsh working environment, and the combination of diversified superior properties (high transparency, flexibility, thermal conductivity, regulable electronic properties, etc.) enables it to be used for wider applications. The high surface area and conductivity make graphene an ideal material for sensing. Formed as overlapping platelets, graphene can be used for early prediction tool towards danger rating and the early warning of microcracks prior to a material's failure by recently developed method of variable structural colouration [1]. Before designing and manufacturing of wide spectra of devices and structures in which graphene can be used, it is preferable to investigate and model first the behaviour of stresses in such kind of structures.

Molecular dynamic simulations have been widely used to predict the fundamental mechanical and electrical properties of materials at nano-scale, for example, bi-layer graphene [2] or for graphene–epoxy nanocomposites [3]. As it is seen from the recent review article on mechanical properties of graphene and graphene-based nanocomposites [4], the presence of graphene even at very low loadings can provide significant reinforcement to the final material. Also, there is noted, that it is easier for the graphene flake to become de-attached when compressive forces are applied to the polymer beam, than tension ones. Examples and results for the mapping of monolayered graphene on different polymer substrate in tension and compression by experimental work and shear-lag model are presented in [5, 6].

Adding of graphene nanosheets in composites enhanced the capacity and performance of lithium-ion batteries made of the graphene-filled layered composite electrodes [7]. The properties of the Sn-based nanocomposites reinforced by different graphene nanosheets volume fractions were predicted by Pouyanmehr et al. [7], using the Mori-Tanaka micromechanical model. It was found that the diffusion induced stresses in the nanocomposite electrodes are very sensitive to the GNS dispersion type and aligning. The last one can reduce the peak stresses in both current collector and active plate and therefore, postpone the common mechanical failures in the electrodes of lithium-ion batteries during charging operation [7].

Actually, the experimental data (in stresses and strains) for the reaction of the layered nanocomposite (two, three or more layers of different materials, at least one of which is in the nanoscale), subjected to a combined load, are quite scarce. The available experimental studies [8-16, 33] are mainly for bilayer structures and for the graphene/PMMA material combination. Experimental data on the distribution of stresses and/or strains in two- or three-layer nanocomposites subjected to tension are given only in [8-9,12-16], and only [8] and [14-16] refer to a combination of graphene with substrates other than PMMA, and [9] for a combination of non-graphene 2D nanomaterial (tungsten disulphide) WS_2 with PMMA and poly(vinyl alcohol) (PVA). The need for experimental data is indisputable, on the one hand - because of the validation of model results, and on the other - the physical, chemical and

Published online: March 05 2022

other macro characteristics of the substances used in a model structure enter as input data in each model type. As can be seen in the review by Young et al, 2012 [17], experimental data on the distribution of deformations in monolayer (or more) graphene coated or embedded to enhance the strength of the polymer substrate itself can be obtained with Raman spectroscopy. In the work of Zhao et al. 2019 [11] a systematic investigation of the strength of monolayer graphene via the application of Raman spectroscopy and computational quantum mechanical modelling is presented. It is found that the strength of flakes tends to decrease as they increase in size. Deformation of the flakes has been shown to occur through interfacial stress transfer from the PMMA substrate via a shear-lag process and relatively narrow monolayer flakes tend to undergo interfacial failure rather than fracture. Apart from graphene, up to the authors' knowledge, the only other experimental data found so far on the distribution of strains in a layer of another nanomaterial (WS_2) were published last year [9].

Modelling at the macro level (stresses, strains, moments) of the behaviour of such nanocomposites under combined loading is a challenge hitherto taken up only by the finite element method (FEM), implemented by powerful and expensive commercial software packages - ANSYS, Abaqus, COSMOS etc. [18-22]. However, these software packages also require knowledge of the macro characteristics of each layer of the nanocomposite (Young's and Poisson's moduli, maximum shear / tensile strength), as well as other coefficients and parameters related to external influences on it (under heat load, for example, it is necessary to know the coefficient of thermal expansion of each layer).

Analytical methods and models for describing the behaviour of layered nanocomposites under combined loading at the macro level are few. Leading models are one-dimensional (e.g., shear-lag, non-linear shear lag) and are used mainly in two-layer structures containing graphene [8-11, 14]. Two-dimensional analytical solutions (continuum mechanics, plate theory) are also known, which refer to mechanical and / or thermal loading in layered composite structures (single lap-joint, double lap joint) [23-25], but not to those with included 2D nano additives or layers.

It is interesting, that to the best of authors' knowledge, there are still not published results for two-dimensional modelling of mechanical response of graphene monolayer, coated or embedded in the polymer substrate, which is axially loaded on tension. Although monolayer graphene has a two-dimensional planar structure, the results of [6] show, that 1D shear lag model successfully can be used to describe the behaviour of graphene strain and interface shear stress under tension load. The application of two-dimensional stress function method, combined with minimization of complementary strain energy functional and developing of governing ordinary differential equations (ODE) for 2 or even 4 unknown functions, to obtain two-dimensional stresses in adhesive bonded lap joints or laminates, can be seen in [26-31]. Almost all results obtained are in closed form solutions (analytical) and applied for structures geometry in mm. In [31] the abovementioned two-dimensional approach is applied to a single lap-joint and the obtained ODE of forth order is relative to only one unknown function - longitudinal (axial) stress in the upper joint adherend.

That encouraged the authors of this work to check the availability of the two-dimensional stress function method and minimization of complementary strain energy functional to a nanostructure graphene-SU-8-Polyethylene terephthalate [32]. After a first successful attempt, here, in this work, we test this method to another case study, which gives another type of analytical solution, different from that in [32]. All axial, shear and peel stresses and strains in the axially loaded nanocomposite structure graphene-SU-8-PMMA are calculated on the base of the new solution and presented graphically as 2D surfaces. The validity of the obtained results for strain in graphene layer here is verified by experimental results for graphene strain (Raman spectroscopy) and shear-lag model predictions, both obtained by Gong in his PhD thesis [6].

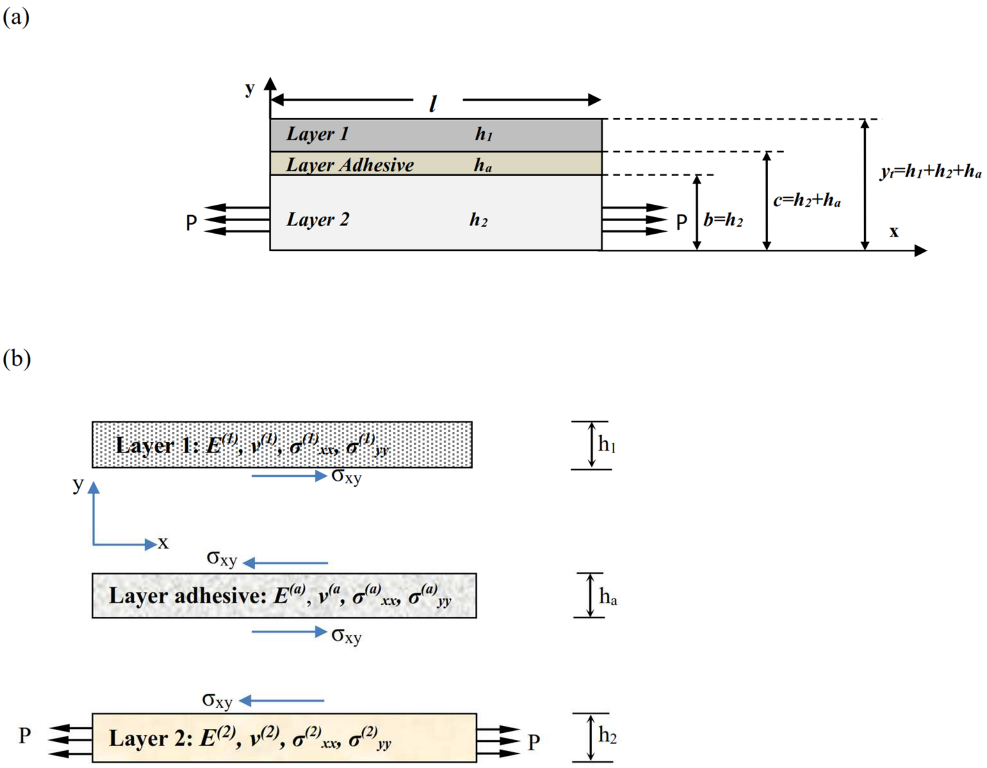

Fig. 1. Model of RVE of three-layered adhesive bonded graphene/polymer nanocomposite structure (a), and schematic configuration of the structure (b).

2. Statement of the Problem and Developed Analytical Solution

Usually, the graphene flake is embedded in the polymer matrix, which can increase the strength and toughness of the respective nanocomposite. In this study, a representative volume element (RVE) of the monolayered graphene/SU-8/PMMA nanocomposite structure (Fig.1, (a)) is considered. The axial tensile force P is applied to the PMMA layer, h_i, $(i=1,2,a)$ are the thicknesses of the graphene, PMMA and adhesive (SU-8) layers. The coordinate system Oxy is placed at the left end of the structure with a length l, the y-coordinates for the layers are noted with $b=h_2, c=h_2+h_a, y_t=h_2+h_a+h_1$.

A detailed description and development of full two-dimensional stress function method is given in our previous work, for the axially loaded nanocomposite structure graphene-SU-8-Polyethylene terephthalate (PET) [32]. For the case of brevity, here only a part of the equations is presented. The initial assumptions of 2D stress-function variational method for the considered nanocomposite structure consist in the following [32]:

1. The axial stresses in the layers are assumed to be functions of axial coordinate x only. Physically, no load transfer occurs over the layers ends.
2. In the adhesive interface layer the axial stress $\sigma_{xx}^{(a)} \equiv 0$ is neglected.
3. All stresses in the layers (axial, normal (peel) and shear stresses) are determined under the assumption of the plane stress formulation (standard constitutive strain-stress equations from 2D elasticity theory).

The boundary and continuity conditions for two-dimensional stresses in the layers in Fig. 1, (b) are as follows:

$$\sigma_{xx}^{(1)}=\begin{cases}0 & \text{if } x=0\\ 0 & \text{if } x=l\end{cases},\qquad \sigma_{xy}^{(1)}=\begin{cases}0 & \text{if } x=0\\ 0 & \text{if } x=l\end{cases},\qquad y\in[c,y_t] \tag{1}$$

$$\sigma_{yy}^{(1)}=\begin{cases}0 & \text{if } y=y_t\\ \sigma_{yy}^{(a)} & \text{if } y=c\end{cases},\qquad \sigma_{xy}^{(1)}=\begin{cases}0 & \text{if } y=y_t\\ \sigma_{xy}^{(a)} & \text{if } y=c\end{cases},\qquad x\in[0,l] \tag{2}$$

$$\sigma_{xx}^{(a)}=\begin{cases}0 & \text{if } x=0\\ 0 & \text{if } x=l\end{cases},\qquad \sigma_{xy}^{(1)}=\begin{cases}0 & \text{if } x=0\\ 0 & \text{if } x=l\end{cases},\qquad y\in[b,c] \tag{3}$$

$$\sigma_{yy}^{(a)}=\begin{cases}\sigma_{yy}^{(1)} & \text{if } y=c\\ \sigma_{yy}^{(2)} & \text{if } y=b\end{cases},\qquad \sigma_{xy}^{(a)}=\begin{cases}\sigma_{xy}^{(1)} & \text{if } y=c\\ \sigma_{xy}^{(2)} & \text{if } y=b\end{cases},\qquad x\in[0,l] \tag{4}$$

$$\sigma_{xx}^{(2)}=\begin{cases}\sigma_0 & \text{if } x=0\\ \sigma_0 & \text{if } x=l\end{cases},\qquad \sigma_{xy}^{(2)}=\begin{cases}0 & \text{if } x=0\\ 0 & \text{if } x=l\end{cases},\qquad y\in[0,b] \tag{5}$$

$$\sigma_{yy}^{(2)}=\begin{cases}\sigma_{yy}^{(a)} & \text{if } y=b\\ 0 & \text{if } y=0\end{cases},\qquad \sigma_{xy}^{(2)}=\begin{cases}\sigma_{xy}^{(a)} & \text{if } y=b\\ 0 & \text{if } y=0\end{cases},\qquad x\in[0,l] \tag{6}$$

where $\sigma_{xx}^{(i)}, \sigma_{xy}^{(i)}, \sigma_{yy}^{(i)}$ are the axial, shear and peel stresses for the three layers, $\sigma_0=P/h_2$ in (Pa), is the external applied tension load to the lower layer.

The stresses in each layer of the RVE of graphene-SU-8-PMMA nanocomposite structure can be expressed in terms of a single stress potential function (the axial stress of the graphene layer is noted with σ_1, function only of x) and its first and second derivatives [32], as follows:

$$\sigma_{xx}^{(1)}=\sigma_1(x)=\sigma_1,\qquad \sigma_{yy}^{(1)}=\frac{1}{2}(y-y_t)^2\sigma_1'',\qquad \sigma_{xy}^{(1)}=(y_t-y)\sigma_1' \tag{7}$$

$$\sigma_{xx}^{(a)}\equiv 0,\qquad \sigma_{yy}^{(a)}=\left[\frac{b^2}{2}+b(c-y)\right]\sigma_1'',\qquad \sigma_{xy}^{(a)}=b\sigma_1' \tag{8}$$

$$\sigma_{xx}^{(2)}=\sigma_0-\rho\sigma_1,\qquad \sigma_{yy}^{(2)}=\frac{-\rho}{2}\left[y^2-y(y_t+h_a)\right]\sigma_1'',\qquad \sigma_{xy}^{(2)}=\rho y\sigma_1',\quad \text{where}\quad \rho=\frac{h_1}{h_2} \tag{9}$$

Likewise, similar formulas can be derived for the deformations (axial, normal and shear strains) in each of the layers in Fig. 1, (a), based on the constitutive equations of mechanics:

$$\varepsilon_{xx}^{(i)}=\frac{\sigma_{xx}^{(i)}}{E^{(i)}}-\frac{\nu^{(i)}\sigma_{yy}^{(i)}}{E^{(i)}},\qquad \varepsilon_{yy}^{(i)}=-\frac{\nu^{(i)}\sigma_{xx}^{(i)}}{E^{(i)}}+\frac{\sigma_{yy}^{(i)}}{E^{(i)}},\qquad \varepsilon_{xy}^{(i)}=\frac{\left(1+\nu^{(i)}\right)\sigma_{xy}^{(i)}}{E^{(i)}},\ (i=1,2,a) \tag{10}$$

where $E^{(i)}$ and $\nu^{(i)}$ are the Young's modulus and Poisson's ratio of the layers.

Next, the complementary strain energy W_i has to be calculated, integrating by y in each layer $(i=1,2,a)$, as follows:

$$\begin{aligned} W_1&=\frac{1}{2}\int_0^l\int_c^{y_t}\left[\sigma_{xx}^{(1)}.\varepsilon_{xx}^{(1)}+\sigma_{yy}^{(1)}.\varepsilon_{yy}^{(1)}+2.\sigma_{xy}^{(1)}.\varepsilon_{xy}^{(1)}\right]dydx,\\ W_a&=\frac{1}{2}\int_0^l\int_b^{c}\left[\sigma_{xx}^{(a)}.\varepsilon_{xx}^{(a)}+\sigma_{yy}^{(a)}.\varepsilon_{yy}^{(a)}+2.\sigma_{xy}^{(a)}.\varepsilon_{xy}^{(a)}\right]dydx,\\ W_2&=\frac{1}{2}\int_0^l\int_0^{b}\left[\sigma_{xx}^{(2)}.\varepsilon_{xx}^{(2)}+\sigma_{yy}^{(2)}.\varepsilon_{yy}^{(2)}+2.\sigma_{xy}^{(2)}.\varepsilon_{xy}^{(2)}\right]dydx \end{aligned} \tag{11}$$

Using Eqs. (7÷9) and plane stress formulation for deformations in layers Eq. (10), finally, the total strain energy W of the nanocomposite structure can be re-written as:

$$W=\frac{1}{2}\int_0^l\left[D_1(\sigma_1)^2+D_2\left(\sigma_1^{''}\right)^2+D_3\left(\sigma_1\sigma_1^{''}\right)+D_4\left(\sigma_1^{'}\right)^2+D_5(\sigma_1)+D_6\left(\sigma_1^{''}\right)+D_7\right]dx=\ldots=\frac{1}{2}\int_0^l\Phi\left(x,\sigma_1,\sigma_1^{'},\sigma_1^{''}\right)dx \quad (12)$$

The minimum of the functional Φ in Eq. (12) can be found according to the Euler-Lagrange equation of the variational calculus as in [31]. This leads to the following ODE of 4th order in respect to the axial stress of the graphene layer σ_1, with constant coefficients D_i:

$$2D_2\sigma_1^{IV}+(2D_3-2D_4)\sigma_1^{''}+2D_1\sigma_1+D_5=0 \quad (13)$$

The coefficients D_i depend on the material properties thicknesses and material properties of the structure layers and on the magnitude of applied static tensile load too - $h_i, E^{(i)}, \nu^{(i)}, \sigma_0$, as follows:

$$D_1=\frac{h_1}{E^{(1)}}+\frac{h_2\rho^2}{E^{(2)}} \quad (14)$$

$$D_2=\frac{h_1^5}{20E^{(1)}}+\frac{h_1^2h_2}{120E^{(2)}}\left[6h_2^2-15h_2(y_t+h_a)+10(y_t+h_a)^2\right]+\frac{h_1^2h_a}{12E^{(2)}}\left[3h_1^2+6h_1h_a+4h_a^2\right] \quad (15)$$

$$D_3=-\frac{\nu^{(1)}h_1^3}{3E^{(1)}}-\frac{\rho\nu^{(2)}h_1h_2\left[2h_2-3(y_t+h_a)\right]}{6E^{(2)}} \quad (16)$$

$$D_4=\frac{2}{3}\frac{\left(1+\nu^{(1)}\right)h_1^3}{E^{(1)}}+\frac{2}{3}\frac{\left(1+\nu^{(2)}\right)}{E^{(2)}}h_1^2h_2+\frac{2\left(1+\nu^{(a)}\right)h_1^2h_a}{E^{(2)}} \quad (17)$$

$$D_5=-\frac{2h_2\rho\sigma_0}{E^{(2)}} \quad (18)$$

The discriminant of the respective characteristic equation of Eq. (13) can be positive or negative, so the roots can be real, complex or mixed. The sign of the discriminant depends on the thicknesses and material properties of the structure layers, e.g from coefficients $D_i, i=1\div 5$, but not depend on the external tensile load σ_0. The characteristic equation of the homogeneous Eq. (13) is $\lambda^4+\left[(D_3-D_4)/D_2\right]\lambda^2+(D_1/D_2)=0$. If $(D_3-D_4)/D_2<0$, $D_1/D_2>0$ and $\left[(D_3-D_4)/D_2\right]^2-4(D_1/D_2)>0$, for the chosen geometry and materials in the next Section these inequalities are fulfilled and obtained four roots are real, in contrast to the complex roots in [32]. Then, the new general analytical solution in the case of four real roots of Eq. (13) for the axial stress in the graphene layer will be:

$$\sigma_1=C_1\cdot\exp(\lambda_1\cdot x)+C_2\cdot\exp(\lambda_2\cdot x)+C_3\cdot\exp(\lambda_3\cdot x)+C_4\cdot\exp(\lambda_4\cdot x)-A \quad (19)$$

where $C_1\div C_4$ are the integration constants obtained satisfying the boundary conditions (see [32]), and the constant $A=D_5/2D_1$ is the partial solution of the non-homogeneous ODE - Eq. (13). As it can be seen, the general solution – Eq. (19), will depend also on the external static tensile load σ_0. After obtaining the solution for σ_1, all stresses and deformations in the layers (axial, normal (peel) and shear) can be easily determined as functions of σ_1 and their derivatives from Eqs. (7÷10).

3. Results and Comparison of Model Strain in Graphene with Shear Lag Method and Experimental Data of Gong

The geometrical and mechanical characteristics of the considered structure (Fig. 1(a)) graphene flake/SU8/PMMA, are taken from [6] as: $l=12\cdot10^{-6}$m, $\sigma_0=P/h_2=1.5.10^7$Pa, $h_1=0.35\cdot10^{-9}$m, $h_2=2\cdot10^{-6}$m, $h_a=1\cdot10^{-8}$m, $E^{(1)}=1\cdot10^{12}$Pa, $E^{(2)}=3.5\cdot10^9$Pa, $E^{(a)}=2\cdot10^9$Pa, $\nu^{(1)}=0.13$, $\nu^{(2)}=0.35$, $\nu^{(a)}=0.22$. For the chosen geometry and materials, and for the above-mentioned conditions for the coefficients in the characteristic equation, four real roots $\lambda_{1,2}=\pm3.651.10^6$ m^{-1}, $\lambda_{3,4}=\pm3.352.10^6$ m^{-1} are obtained. As it was shown in section 2, all stresses and strains in the layers of the nanocomposite graphene flake/SU8/PMMA are expressed by Eqs. (7÷10) for σ_1 and their first and second derivatives, satisfying the contact conditions in Eqs. (1÷6) for the shear and peel stresses between the common boundaries of the layers and the conditions for stress free surfaces of shear and peel stresses. All calculations are performed on Mathcad Prime, all graphics are created with Sigma Plot, v.13. In Figs. 2 to 4 the behaviour of all calculated stresses (axial, shear and peel) for every layer is illustrated. In Figs. 5 to 7 the respective strains (deformations) in the layers are presented for $\sigma_0=P/h_2=1.5.10^9$Pa, for the needs of comparison of our results for graphene strain with experimental and shear-lag model data in [6].

The axial stresses in Figs. 2÷4 are non-linear functions of the axial coordinate x in graphene and PMMA layers and is 0 in the adhesive layer (model assumption in [32]). The normal (peel) stresses are non-linear functions of x in all layers and quadratic functions of y in the layer graphene and PMMA, but linear function of y in the adhesive. Shear stresses also are non-linear functions of x in all layers and linear functions of y in the layers graphene and PMMA. Regarding to the model strains (Eqs. (10)), the axial and peel strains are quadratic functions of y in graphene and PMMA layers and linear functions in the adhesive layer, being also non-linear functions of x in all layers. The shear strains are linear by y in graphene and PMMA layers and non-linear functions of x in all layers.

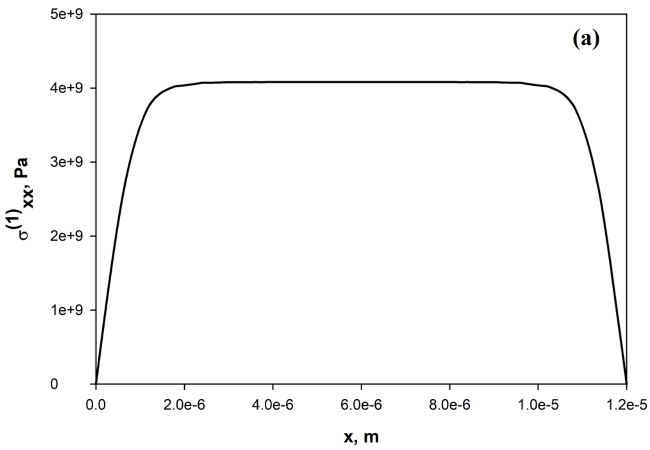

(a)

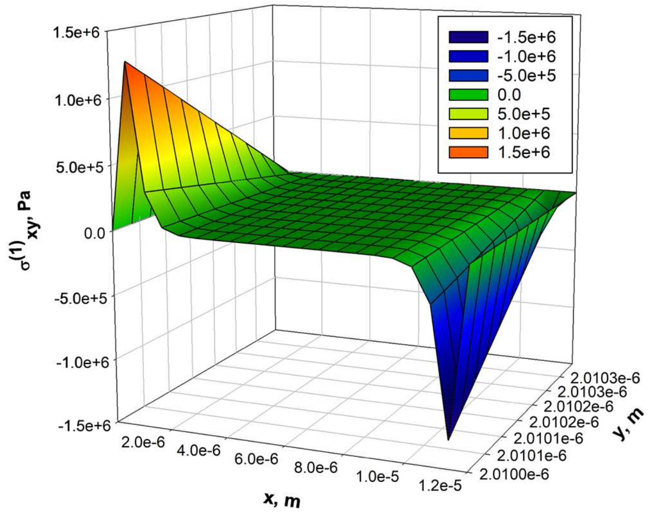

(b)

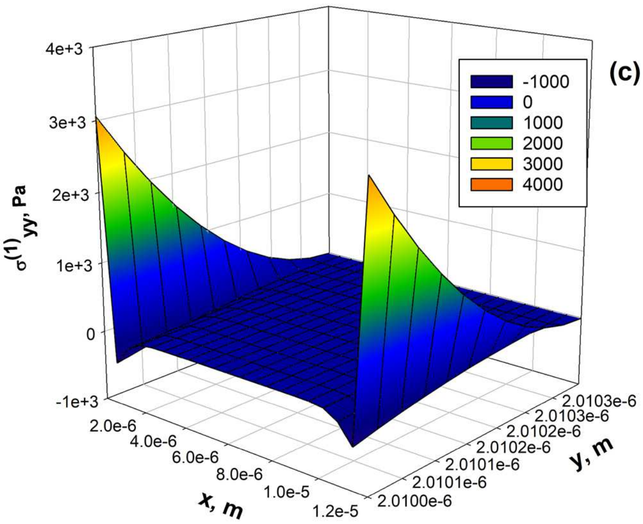

(c)

Fig. 2. Axial $\sigma_{xx}^{(1)}$ (a), shear $\sigma_{xy}^{(1)}$ (b) and peel $\sigma_{yy}^{(1)}$ (c) surfaces of stresses in the graphene layer 1.

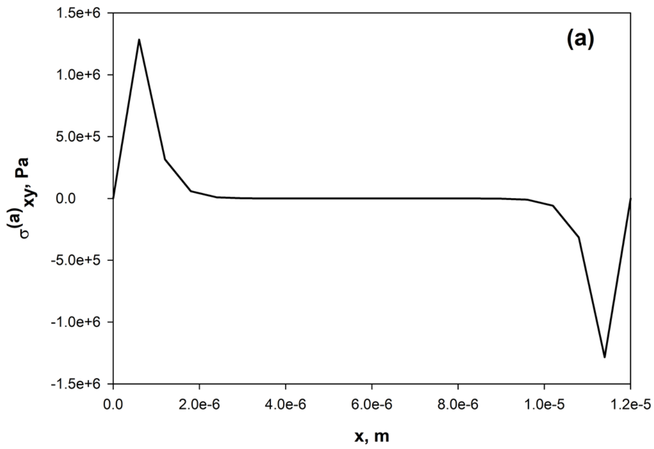

(a)

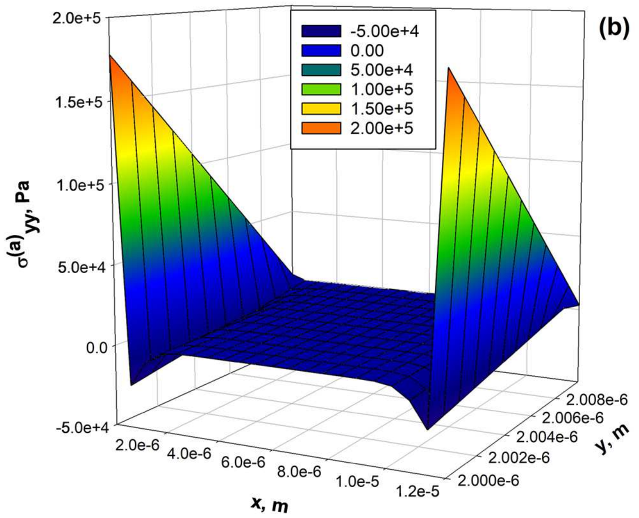

(b)

Fig. 3. Shear $\sigma_{xy}^{(a)}$ (a) and peel $\sigma_{yy}^{(a)}$ (b) surfaces of stresses in the adhesive layer.

An additional qualitative validation of the results for all stresses calculated and presented in Figs. 2÷4 can be seen in [34]. In the work of Ghoddous [34], two-dimensional elasticity theory is applied and analytical closed-form solutions for shear and peel stresses are obtained, for a stiffened lap joint under uniform tensile load. Our results for the normal stresses in the layers show the same tendency as Ghoddous' ones: the normal stress between the bottom layer and the adhesive dominates over the same one between the top layer and the adhesive. Also, the behavior of the shear stresses is the same as in [34], with peaks close to the ends of the overlap zone; in the rest region of the zone it is approximately 0. The results in [34] are compared with FEM and have shown a very good agreement for the investigated joint materials (Aluminum for the top and bottom layers and epoxy adhesive for the middle layer).

As is seen from Figs. 5÷7, the shape of the surfaces for the shear strains in the layers follows the shapes of the respective stresses. A similar type of graphics results for strains are obtained and presented in [24] for adhesively bonded single lap joints. In [24, Fig. 25] the analytical results for axial and normal strains in the first layer (upper adherent of the joint) have been compared with the results by FEM simulation and the comparison shows "fairly good agreement".

It has to be noted that, because of the differences in the structure properties and geometry here and those studied in [32] - graphene/SU-8/PET, the solution σ_1 and respectively, stresses here are completely different. Here, in Eq. (19) the solution is expressed with hyperbolic cosines and sines, because the discriminant of the characteristic equation of Eq. (13) is positive and the four roots are real numbers. In [32], the chosen polymer layer is PET, and also, the thicknesses of the layers are quite different and influence the type of the solution. In [32] the discriminant is negative, the roots are complex, and the solution is represented as a combination of cosines and sines. All this reflects on the shapes of the surfaces for shear and peel stresses in the structure layers – they are smoother and well-covered than these, presented here. For the comparison purposes of our predictions results for the strain in the graphene layer, with analogous results of Gong [6] – experimental data and model shear-lag predictions, here thicknesses of the layers are chosen to be equal to those in the experiment in [6]. Figure 8 shows the comparison of the model predictions for graphene axial strain $\varepsilon_{xx}^{(1)}$ with the experimental data (Raman spectroscopy) and shear lag predictions [6] for the considered structure at external strain loading of 0.4% and 0.6%.

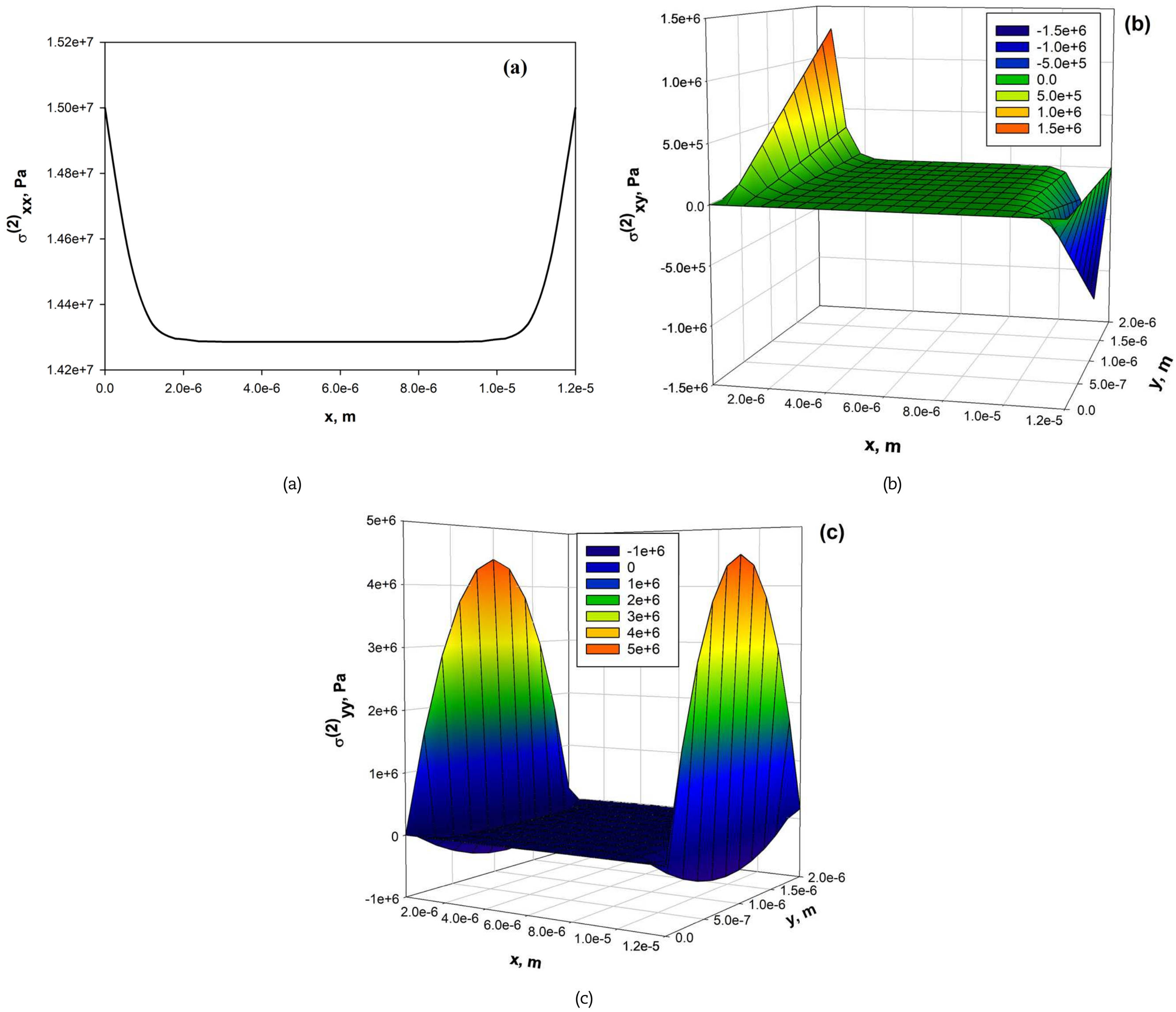

Fig. 4. Axial $\sigma_{xx}^{(2)}$ (a), shear $\sigma_{xy}^{(2)}$ (b) and peel $\sigma_{yy}^{(2)}$ (c) graphics of stresses for the PMMA layer.

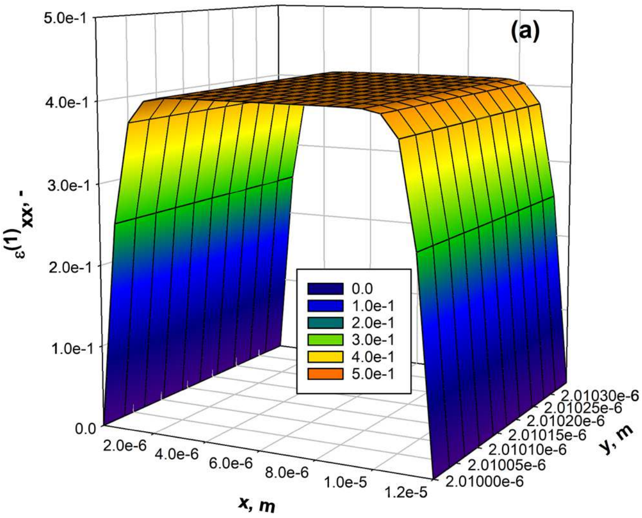

(a)

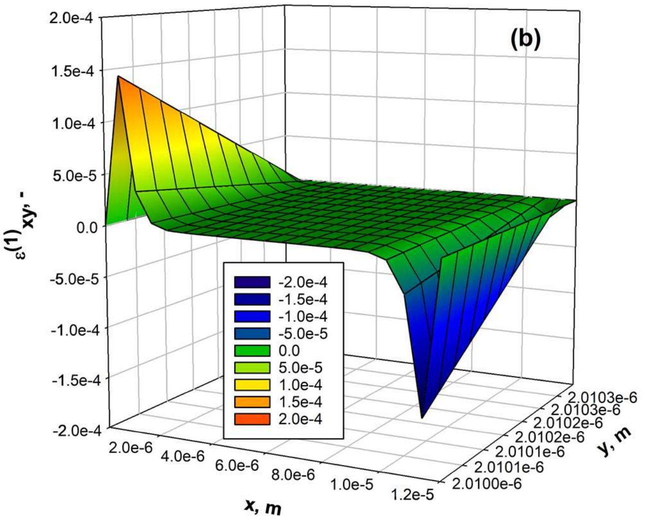

(b)

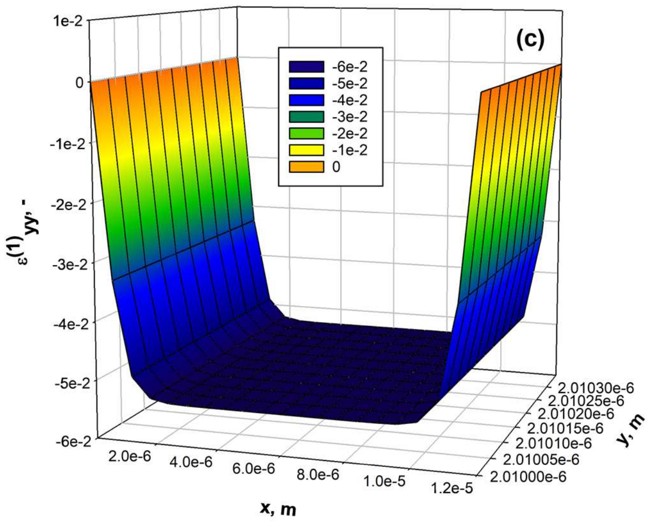

(c)

Fig. 5. Axial $\varepsilon_{xx}^{(1)}$ (a), shear $\varepsilon_{xy}^{(1)}$ (b) and peel $\varepsilon_{yy}^{(1)}$ (c) surfaces of strains in the graphene layer 1.

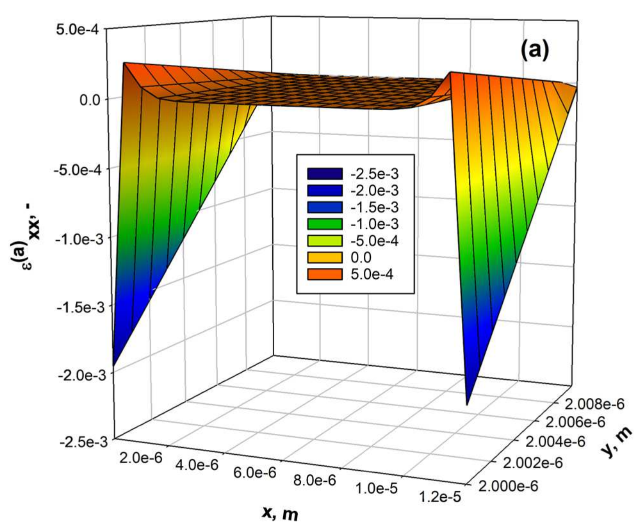

(a)

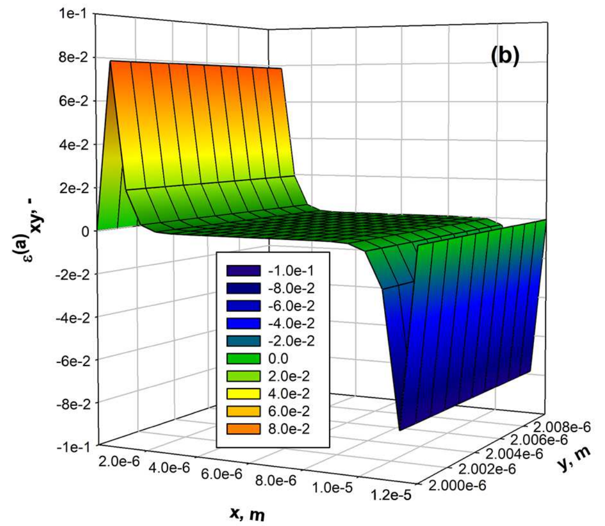

(b)

Fig. 6. Axial $\varepsilon_{xx}^{(a)}$ (a), shear $\varepsilon_{xy}^{(a)}$ (b) and peel $\varepsilon_{yy}^{(a)}$ (c) surfaces of strains in the adhesive layer.

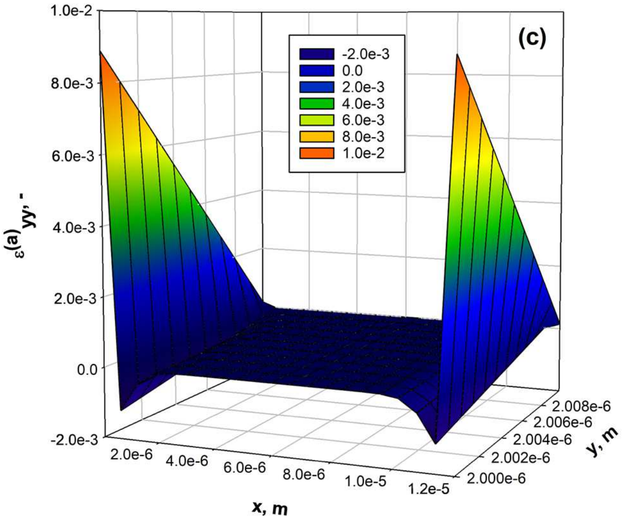

(c)

Fig. 6. Continued.

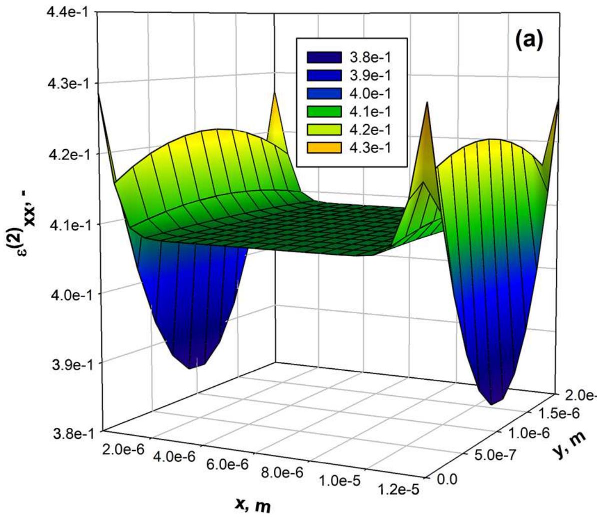

(a)

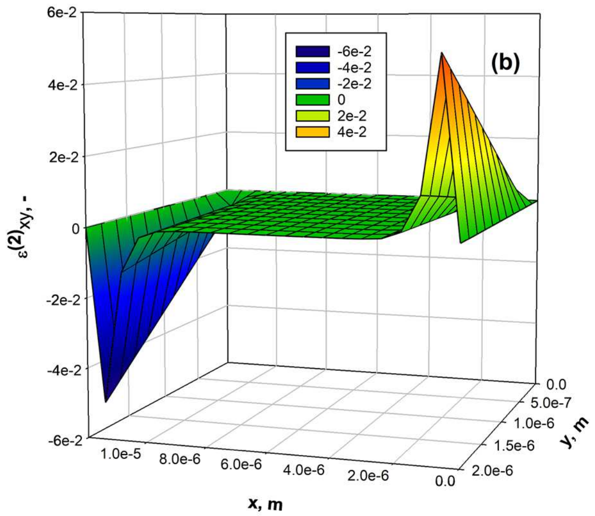

(b)

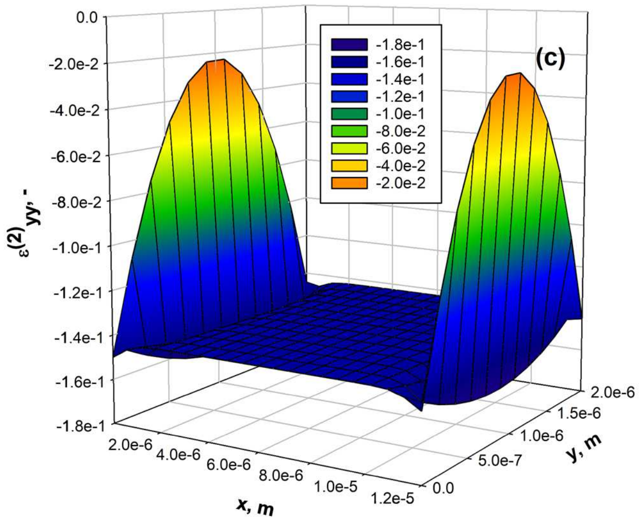

(c)

Fig. 7. Axial $\varepsilon_{xx}^{(2)}$ (a), shear $\varepsilon_{xy}^{(2)}$ (b) and peel $\varepsilon_{yy}^{(2)}$ (c) surfaces of strains for the second (PMMA) layer.

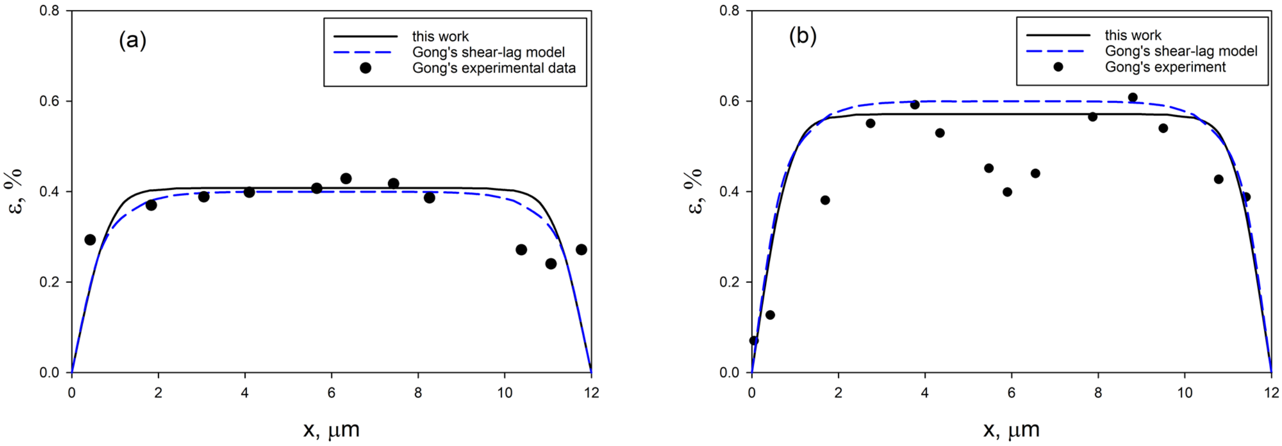

(a) (b)

Fig. 8. Comparison of our model predictions for the graphene axial strain $\varepsilon_{xx}^{(1)}$ with Gong's shear lag model and experimental Raman spectroscopy data [6]: (a) for external strain of 0.4%, (b) – for external strain of 0.6%.

The absolute mean relative error between the experimental data [6] and our results is 10 %, respectively, between shear-lag [6] and our results is 12% for 0.4% external strain. This good agreement supports the validity and power of the two-dimensional stress-function variational method for prediction of stresses and strains in the layers of the considered nanocomposite structure graphene/SU-8/PMMA, subjected to axial loading (tension). The validity of the proposed method is in the elastic region only. For 0.6% external strains (Fig. 8, (b)) both model predictions - our and shear-lag [6], are unable to fit exactly the experimental data of Gong [6]. The explanation of this is the Gong's experimental observation, that some relaxation zone appears between 0.4% and 0.7% external strain, which deform the strain behavior in the middle of the layer. When the matrix strain was increased to 0.6% a different distribution of axial strain in the graphene monolayer was obtained experimentally (Fig.8b). Gong concluded [6] that there appears to be an approximately linear variation of the graphene strain from the edges to the center of the monolayer up to 0.6% strain and a dip in the middle down to around 0.4% strain. In this case it appears that the interface between the graphene and polymer has failed and stress transfer is taking place through interfacial friction. The strain in the graphene does not fall to zero in the middle of the flake, however, showing that the flake remains intact. In support of this claim, one can find another evidence in [33]. Polyzos et al. [33] investigated experimentally the behaviour of stresses and strains in a suspended graphene flake between two PMMA layers subjected by uniaxial deformation. In [33] it is reported that up to 0.8% external deformation, there exists "an evidence, that axial loading of graphene, is always accompanied by the formation of orthogonal wrinkles similar to what is observed when a thin-macroscopic- membrane is stretched uniaxially". It was mentioning also that the constrains in their research method require a linear relationship between stress and strain [33].

In relation with our future plans, the above mentioned validation for the elastic results will encourage us to continue with parametric studies in similar loaded nanocomposite structures, in spite of the fact that the configuration considered is only an idealized model. It allows from obtained closed –form model solutions quickly and easily to obtain results about the load transfer between the layers in such sandwich-type nanocomposites, to investigate the typical distance on which the load transfer happens, as well as to investigate the dependence between the given elastic properties and the geometrical quantities (length and layer thicknesses) and the debonding length in such kind of structures in the elastic region.

4. Conclusions

The two-dimensional stress-function variational method presented has been applied to predict the stresses and strains behaviour in a three-layered graphene/SU-8/PMMA structure, subjected to tensile static load. The resulting differential equation with constant coefficients for the axial stress in graphene as a minimum of the complementary strain energy was derived and solved, at the case of four real roots. Based on it, the analytical expressions of all two-dimensional stresses and strains in the structure layers were found in the new closed-form solutions. The structure's geometry and material properties were included in the coefficients of ODE of forth order and practically determined the type of the solution for axial stress in graphene layer, as well as the type of other stresses/strains in the rest of the layers, too. This reflected on the shapes of the surfaces for shear and peel stresses in the structure layers; for the solution with complex roots [32] they were smoother and well-covered than obtained here for real roots.

The theoretical predictions of 2D stress function variational method and 1D shear lag of Gong [6] for the axial strain of the graphene, and the respective experimental data done by Raman spectroscopy [6], were compared for two values of external strain loading. The comparison showed good agreement between shear-lag [6], our results and the experimental data [6] for the case of 0.4% external strain, with absolute mean relative error up to 10-12%. At 0.6% external strain, the experimental data of Gong for strain in graphene showed that some relaxation zone appears between 0.4% and 0.7% external strain, which deform the strain behaviour in the middle of the graphene layer and clearly constrained application of both shear-lag and our predictions to describe the graphene strain in this zone. Nevertheless, in the elastic region, the proposed 2D stress-function variational method is applicable for fast and easy prediction of the stresses and strains in layered nanostructures.

Author Contributions

All authors planned the scheme, initiated the project, developed the mathematical modeling, examined the theory validation and conducted the numerical tests. The manuscript was written through the contribution of all authors. All authors discussed the results, reviewed, and approved the final version of the manuscript.

Acknowledgments

The authors gratefully acknowledge the Bulgarian National Science Fund for its financial support via the contract for project КП-06-Н57/3/15.11.2021.

Conflict of Interest

The authors declared no potential conflicts of interest concerning the research, authorship, and publication of this article.

Funding

The authors received financial support for the research of this article by the Bulgarian National Science Fund by the contract No. КП-06-Н57/3/15.11.2021.

Data Availability Statements

The datasets generated and/or analyzed during the current study are available from the corresponding author on reasonable request.

Nomenclature

$A=D_5/2D_1$	Constant in Eq. (19), partial solution of Eq. (13)	W_i, W	Local and total complementary strain energy in Eqs. (11-12)
$b=h_2$	Thickness of Layer 2 in Fig. 1 [m]	$\varepsilon_{xx}^{(i)},\varepsilon_{xy}^{(i)},\varepsilon_{yy}^{(i)}$	two-dimensional deformations (strains) in the layer [-]
C_i	Integration constants in the model solution for axial stress in the first layer - Eq. (19), i=1÷4	λ_i	Roots of characteristic equation of Eq. (13), i=1÷4 $[m]^{-1}$
$c=h_2+h_a$	Thickness of Layer 2 in Fig.1 [m]	$\nu^{(i)}$	Poisson's ratio of the layers, (i=1,2,a) [-]
D_i	Constants in Eq. (13), i=1÷5	$\rho = h_1 / h_2$	Ratio of thicknesses [-]
$E^{(i)}$	Young's modulus of the layers, i=1,2,a [GPa]	$\sigma_{xx}^{(i)},\sigma_{xy}^{(i)},\sigma_{yy}^{(i)}$	Two-dimensional stresses in the layers, (i=1,2,a) [Pa]
h_i	Thickness of the layers in Fig. 1, [m]	$\sigma_1', \sigma_1'', \sigma_1^{IV}$	First, second and forth derivative of axial stress in 1st layer
l	Structure length in Fig. 1 [m]	$\sigma_0 = P / h_2$	External axial tensile load, applied on the 2-nd layer [Pa]
P	Tensile axial force in Fig. 1 [Pa.m]	σ_1	Axial stress in the layer 1 (graphene) [Pa]
x, y	Coordinate axes in Fig. 1 [m]	$\sigma_{xx}^{(2)} = \sigma_0 - \rho\sigma_1$	Axial stress in Layer 2 (PMMA) [Pa]
$y_t=h_1+h_2+h_a$	Thickness if the whole structure in Fig. 1 [m]	Φ	Functional in Eq. (12)

References

[1] Deng, Y.H., Gao, S.L., Liu, J.W., Gohs, U., Mäder, E., Heinrich, G., Variable structural colouration of composite interphases, *Materials Horizons*, 4(3), 2017, 389-395.
[2] Wang, L., Zhang, Q., Elastic behavior of bilayer graphene under in-plane loadings, *Current Applied Physics*, 12(4), 2012, 1173-1177.
[3] Rahman, R., Haque, A., Molecular modeling of crosslinked graphene–epoxy nanocomposites for characterization of elastic constants and interfacial properties, *Composites Part B: Engineering*, 54, 2013, 353-364.
[4] Papageorgiou, D.G., Kinloch, I.A., Young, R.J., Mechanical properties of graphene and graphene-based nanocomposites, *Progress in Materials Science*, 90, 2017, 75-127.
[5] Jiang, T., Huang, R., Zhu, Y., Interfacial Sliding and Buckling of Monolayer Graphene on a Stretchable Substrate, *Advanced Functional Materials*, 24(3), 2014, 396-402.
[6] Gong, L., *Deformation micromechanics of graphene nanocomposites*, Ph.D. Thesis, School of Materials, Faculty of Engineering and Physical Sciences, The University of Manchester, Manchester, UK, 2012.
[7] Pouyanmehr, R., Hassanzadeh-Aghdam, M.K., Ansari, R., Effect of graphene nanosheet dispersion on diffusion-induced stresses in layered sn-based nanocomposite electrode for lithium-ion batteries, *Mechanics of Materials*, 145, 2020, 103390.
[8] Bronsgeest, M.S., Bendiab, N., Mathur, S., Kimouche, A., Johnson, H.T., Coraux, J., Pochet, P., Strain relaxation in CVD graphene: wrinkling with shear lag, *Nano letters*, 15(8), 2015, 5098–5104.
[9] Wang, F., Li, S., Bissett, M.A., Kinloch, I.A., Li, Z., Young, R.J., Strain engineering in monolayer WS_2 and WS_2 nanocomposites, *2D Materials*, 7(4), 2020, 045022.
[10] Zhao, X., Papageorgiou, D.G., Zhu, L., Ding, F., Young, R.J., The strength of mechanically-exfoliated monolayer graphene deformed on a rigid polymer substrate, *Nanoscale*, 11(30), 2019, 14339-14353.
[11] Wang, G., Dai, Z., Liu, L., Hu, H., Dai, Q., Zhang, Z., Tuning the Interfacial Mechanical Behaviors of Monolayer Graphene/ PMMA Nanocomposites, *ACS Applied Materials and Interfaces*, 8(34), 2016, 22554–22562.
[12] Anagnostopoulos, G., Androulidakis, C., Koukaras, E.N., Tsoukleri, G., Polyzos, I., Parthenios, J., Papagelis, K., Galiotis, C., Stress transfer mechanisms at the sub-micron level for graphene/ polymer systems, *ACS Applied Materials and Interfaces*, 7(7), 2015, 4216–4223.
[13] Androulidakis, Ch., Sourlantzis, D., Koukaras, E.N., Manikas, A.C., Galiotis, C., Stress-transfer from polymer substrates to monolayer and few-layer graphenes, *Nanoscale Advances*, 1(12), 2019, 4972-4980.
[14] Li, X., Warzywoda, J., McKenna, G.B., Mechanical responses of a polymer graphene-sheet nano-sandwich, *Polymer*, 55(19), 2014, 4976-4982.
[15] Xu, C., Xue, T., Guo, J., Kang, Y., Qiu, W., Song, H., Xie, H., An experimental investigation on the tangential interfacial properties of graphene: Size effect, *Materials Letters*, 161, 2015, 755-758.
[16] Guo, G., Zhu, Y., Cohesive-Shear-Lag Modeling of Interfacial Stress Transfer Between a Monolayer Graphene and a Polymer Substrate, *Journal of*

Applied Mechanics, 82(3), 2015, 031005.
[17] Young, R.J., Kinloch, I.A., Gong, L., Novoselov, K.S., The mechanics of graphene nanocomposites: A review, *Composites Science and Technology*, 72(12), 2012, 1459–1476.
[18] Dai, G., Mishnaevsky, L., Graphene reinforced nanocomposites: 3D simulation of damage and fracture, *Computational Materials Science*, 95, 2014, 684–692.
[19] Spanos, K.N., Georgantzinos, S.K., Anifantis, N.K., Mechanical properties of graphene nanocomposites: A multiscale finite element prediction, *Composite Structures*, 132, 2015, 536-544.
[20] Peng, Y., Deng, K., Study on the mechanical properties of the novel Sn–Bi/Graphene nanocomposite by finite element simulation, *Journal of Alloys and Compounds*, 625, 2015, 44–51.
[21] Gao, X., Li, C., Song, Y., Chou, T.-W., A continuum mechanics model of multi-buckling in graphene –substrate systems with randomly distributed debonding, *International Journal of Solids and Structures*, 97-98, 2016, 510–519.
[22] Guo, Zh., Song, L., Chai, G.B., Li, Zh., Li, Y., Wang, Zh., Multiscale finite element analyses on mechanical properties of graphene-reinforced composites, *Mechanics of Advanced Materials and Structures*, 26(20), 2019, 1735-1742.
[23] Zhang, Y., Zhou, Z., Tan, Z., Compression Shear Properties of Adhesively Bonded Single-Lap Joints of C/C Composite Materials at High Temperatures, *Symmetry*, 11(12), 2019, 1437.
[24] Zhao, B., Lu, Z-H., A Two-Dimensional Approach of Single-Lap Adhesive Bonded Joints, *Mechanics of Advanced Materials and Structures*, 16(2), 2009, 130–159.
[25] Zhao, B., Lu, Z.-H., Lu, Y.-N., Two-dimensional analytical solution of elastic stresses for balanced single-lap joints—Variational method, *International Journal of Adhesion and Adhesives*, 49, 2014, 115–126.
[26] Allman, D. J., A theory for elastic stresses in adhesive bonded lap joints, *The Quarterly Journal of Mechanics and Applied Mathematics*, 30(4), 1977, 415-436.
[27] Hashin, Z., Analysis of cracked laminates: A variational approach, *Mechanics of Materials*, 4(2), 1985, 121-136.
[28] Shi, Y.P., Cheng, S., Analysis of adhesive-bonded cylindrical lap joints subjected to axial load, *Journal of Engineering Mechanics*, 119(3), 1993, 584-602.
[29] Chen, D., Cheng, Sh., An Analysis of Adhesive-Bonded Single-Lap Joints, *Journal of Applied Mechanics*, 50(1), 1983, 109-115.
[30] Kumar, S., Analysis of tubular adhesive joints with a functionally modulus graded bondline subjected to axial loads, *International Journal of Adhesion and Adhesives*, 29(8), 2009, 785–795.
[31] Kumar, S., Tampi, S., Modeling of single-lap composite adhesive joints under mechanical and thermal loads, *Journal of Adhesion Science and Technology*, 30(7), 2016, 759-783.
[32] Kirilova, E., Petrova, T., Becker, W., Ivanova, J., Mathematical modelling of stresses in graphene polymer nanocomposites under static extension load, *2019 IEEE 14th Nanotechnology Materials and Devices Conference (NMDC)*, Stockholm, Sweden, 2019.
[33] Polyzos, I., Bianchi, M., Rizzi, L., Koukaras, E.N., Parthenios, J., Papagelis, K., Sordan, R., Galiotis, C., Suspended monolayer graphene under true uniaxial deformation, *Nanoscale*, 7(30), 2015, 13033-13042.
[34] Ghoddous, B., Theoretical Analysis of Stress Distribution in Bonded Single Strap and Stiffened Joints, *Latin American Journal of Solids and Structures*, 14(2), 2017, 256-276.

ORCID iD

Tatyana Petrova https://orcid.org/0000-0001-9073-4291
Elisaveta Kirilova https://orcid.org/0000-0002-9984-5067
Wilfried Becker https://orcid.org/0000-0002-1804-236X
Jordanka Ivanova https://orcid.org/0000-0002-5430-9957

How to cite this article: Petrova T., Kirilova E., Becker W., Ivanova J. Two-dimensional Stress and strain Analysis for Graphene-polymer Nanocomposite under Axial Load, *J. Appl. Comput. Mech.*, 8(3), 2022, 1065–1075.
https://doi.org/10.22055/jacm.2022.38834.3292